



FRAGILITY SURFACES FOR EFFICIENT SEISMIC ASSESSMENT OF GRAVITY DAMS VIA SURROGATE MODELING

R.L. Segura⁽¹⁾, J.E. Padgett⁽²⁾ and P. Paultre⁽³⁾

⁽¹⁾ Postdoctoral fellow, Department of Civil and Building Engineering, University of Sherbrooke, Sherbrooke, QC, Canada, Rocio.Lilen.Segura@usherbrooke.ca

⁽²⁾ Associate professor, Department of Civil and Environmental Engineering, Rice University, Houston, TX, USA, jamie.padgett@rice.edu

⁽³⁾ Professor, Department of Civil and Building Engineering, University of Sherbrooke, Sherbrooke, QC, Canada, Patrick.Paultre@usherbrooke.ca

Abstract

The consequences of a dam failure could be significant, both in terms of casualties and/or economic and environmental damage, for which its safety is given highest priority. With the increasing knowledge in seismicity, a growing number of dams fail to meet revised safety criteria that incorporate this new seismic hazard information. In recent years, probabilistic methods, such as fragility analysis, have emerged as a reliable tool for the seismic assessment of dam-type structures. However, given that earthquake shaking represents complex loading to a structure, its characterization with a single seismic intensity parameter might not be enough to define the actual seismic scenario at the dam site. Traditional vulnerability assessment methods develop fragility functions by using a single parameter to relate the level of shaking to the expected damage, which consequently produces a robustness of predictions that is highly dependent on the selected parameter. Conversely, the estimation of the fragility of the system can be potentially improved by increasing the number of parameters; in this way, a more complete description of the properties of ground motions can be obtained. While the use of a vector of intensity measures in fragility modeling has been a well-established notion in the literature, the exploration of its validity and form in the context of predicting dam seismic safety remains scarce.

In order to improve the fragility assessment of such structures, by efficiently characterizing the seismic scenario at the dam site, this study proposes the development of fragility surfaces for dams as a function of two seismic intensity measures. In addition, given the complexity of the finite element models used to describe the real dynamic behavior of the dam-reservoir-foundation system and the computing time required to perform a fully probabilistic analysis, this study proposes the use of a polynomial response surface surrogate model instead. The latter will be used to predict the continuous relative maximum base sliding of the dam to build fragility surfaces and show the effect of the seismic response uncertainty. To do so, it is fundamental to perform an accurate estimate of the seismic demand at the dam site and to generate samplings of the possible system configuration by implementing an adequate design of experiment technique, such as Latin Hypercube Sampling.

The training set for the surrogate model is generated by performing non-linear dynamic analysis of one of the central blocks of the dam, including fluid-structure-foundation interaction. The produced training cases are then used to fit a surrogate model, which seeks to emulate the finite element model output. The predictive capabilities of the surrogate model are evaluated considering local and global goodness-of-fit estimates from 5-fold cross validation. This metamodel is then used to generate fragility point estimates which propagate the uncertainty in the seismic loading by considering a range of usable values to define different possible seismic scenarios. In addition, analytical fragility surfaces are developed by extending the multiple stripes analysis, usually used to fit univariate fragility functions, to the multivariate case. Finally, the comparison between fragility estimates obtained with univariate and bivariate seismic fragility functions will be compared to quantify the discrepancy between the two approaches. The proposed methodology is applied to a case-study dam, a concrete gravity dam located in north-eastern Canada.

Keywords: Fragility surfaces, surrogate model, gravity dams, seismic scenario, seismic intensity measures.

1. Introduction

Dams are one of the most audacious human constructions, considering the social, environmental and economic risks that a work of such magnitude entails. A dam is designed to impound and store water behind it safely throughout its lifetime. Thus, it has to maintain its structural integrity in the face of the different hazards and loading conditions that arise during construction, normal operations, and extreme environmental events. Several dams have experienced rupture (partially or totally) under the effect of exceptional floods,



and to a lesser extent due to earthquakes. In the last years the documented damage caused by seismic events [1, 2] has revealed the vulnerability of these structures whose consequences are catastrophic and expensive. With the increasing knowledge of seismicity, a growing number of dams fail to meet the revised safety criteria that incorporates new seismic hazard information [3]. Consequently, the combination of ageing and its associated problems with new methods for estimating seismic loads and with the increasing demands of society to ensure a high level of safety has resulted in the need to review and upgrade the methods of seismic analysis for dams.

Methods for analyzing the structural response of a dam-reservoir-foundation system rely on deterministic or probabilistic approaches. Deterministic methods are often considered too conservatives [4, 5, 6], therefore, probabilistic approaches are preferred to manage the various sources of uncertainty that may impact the dam performance and decisions related thereto [4]. Within this probabilistic framework, a fragility analysis is a promising alternative, particularly suited to study the seismic vulnerability of structures and to estimate the level of damage likely to be caused by seismic events.

Traditional vulnerability assessment methods develop fragility functions by using a single parameter to relate the level of shaking to the expected damage. Single parameter demand models and fragility curves are highly dependent on the selected seismic intensity measure (IM), which consequently influences the robustness of predictions. However, the estimation of the fragility of the system can be potentially improved by increasing the number of parameters; in this way, a more complete description of the properties of ground motions can be obtained [7]. Consequently, the use of multi-parameter models to predict the response of a certain structure is beginning to be used increasingly [8, 9]. Several authors [10, 11] proposed the idea of vector valued IMs long ago; but there are still gaps in testing or extending the concept especially in the context of dams.

Nevertheless, seismic fragility analysis and vulnerability assessment of key infrastructure elements, often requires a large number of non-linear dynamic analyses of complex finite element models (FEM). The substantial computational time may be reduced using machine learning techniques to develop surrogate or meta-models, which are an engineering method used when an outcome of interest cannot be easily directly measured, so a model of the outcome is used instead [12]. Such a challenge is particularly relevant to the case of large-scale infrastructures, such as dams, subjected to seismic loads. Therefore, to improve the seismic assessment of such structures, this study proposes the development of fragility surfaces as a function of two seismic intensity measures. In addition, given the complexity of the FEM of the dam-reservoir-foundation (DRF) system and the computing time required to perform a fully probabilistic analysis, this study encourages the use of a polynomial response surface surrogate model instead. The latter will be used to predict the continuous relative maximum base sliding of the dam to build fragility surfaces. The proposed methodology is applied to a gravity dam located in north-eastern Canada.

2. Case study description and modeling

As mentioned above, the present study focuses on a particular dam located in north-eastern Canada. It comprises 19 unkeyed monoliths, a maximum crest height of 78 m, and a crest length of 300 m. The width is 4.6 m at the top and 62 m at the base of the largest monolith. The dam rests on a foundation consisting mainly of anorthosite gabbro and granitic gneiss [13], which corresponds to hard rock ($V_{S30} > 1500$ m/s). The dam was chosen for its simple and almost symmetric geometry, as well as for its well-documented dynamic behavior. In addition, forced vibration test results are available for calibration of the dynamic properties of the numerical dam model [13]. The tallest monolith of the dam was considered to be representative of the structure. The dimensions and meshing of the foundation and the reservoir in the finite element model (Fig. 1) were defined consistent with the recommendations of the United States Bureau of Reclamation (USBR) [14]. The FEM was analyzed with the computer software LS-Dyna [15], using the software's explicit solver. The proposed model considers the diverse interactions between the structure, the reservoir and the foundation. The reservoir is modelled with compressible fluid elements, while the concrete body of the dam and the rock foundation were modelled with linear elastic materials. The non-linearities are



concentrated in the model at the base and neck of the dam, and they were introduced in the model in the form of contact surfaces between the dam system components. By modifying the properties of the dam and the foundation materials, the fundamental period of the DRF system was 0.25 s, which matches the fundamental period from a previous model of the same monolith calibrated from in situ forced vibration tests [13]. Further details on the modelling assumptions and the validation of the numerical model can be found in Bernier et al. [16] and Segura et al. [17].

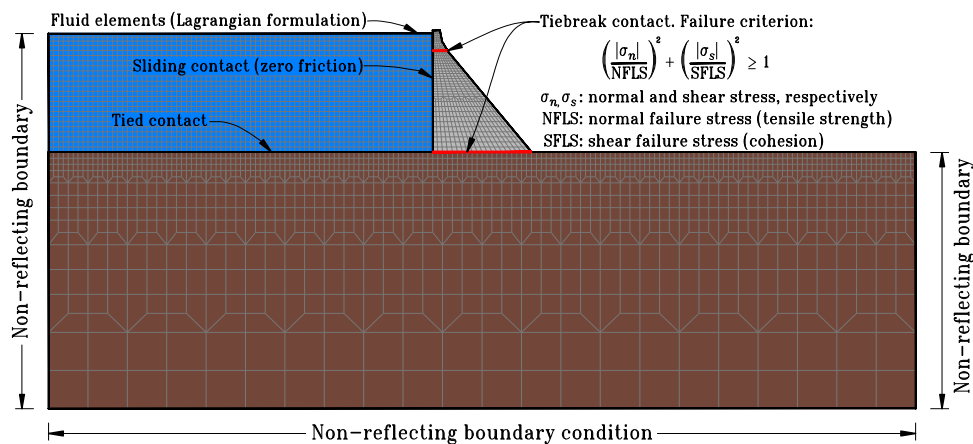


Fig. 1 – Finite element model of the tallest monolith

3. Characterization of the seismic scenario

3.1 Probabilistic seismic hazard analysis – PSHA

Although eastern Canada is located in a stable zone, the occurrence of several major earthquakes in the south-east of the country, has led to the consideration of this area as a moderate seismic zone. The most recent hazard model, on which the seismic provisions of the 2015 National Building Code of Canada (NBCC) [18] are based, comprises four components, one for each quadrant (north-west, south-west, northeast and south-east), to reduce computational burden [19]. In this context, an updated hazard model for the south-eastern quadrant was considered for this study, using three sub-models, distinguished primarily as the historical cluster (H2), regional seismotectonic (R2) and a hybrid approach (HY) between H2 and R2. The adopted weights were 0.4 for both H2 and HY and 0.2 for R2. The empirical ground motion models were provided in the form of look-up tables (based on Atkinson and Adams [20]) to be used with the considered sources.

A probabilistic seismic hazard analysis (PSHA) was then performed at the dam site using the open-source software OpenQuake [19], which features the aforementioned 2015 NBCC hazard model, as part of a project at the Global Earthquake Model (GEM) Foundation, using information provided by the Geological Survey of Canada (GSC). The hazard levels were defined in terms of spectral acceleration at the fundamental period of the structure ($Sa(T_1)$) to conveniently cover the range of spectral accelerations corresponding to return periods from 700 to 30000 years. To identify the earthquake scenarios with the greatest contribution to the overall seismic hazard, disaggregation was performed for the considered hazard levels. The disaggregation results are showed that for low $Sa(T_1)$ values, events of magnitudes between 5.0 and 6.0 and distances between 15 km and 85 km are predominant at the dam site, while for high $Sa(T_1)$ values, contributions to the hazard are mainly from distances between 0 km and 45 km and magnitudes between 6.0 and 7.5. Further details regarding the procedure used to perform the PSHA can be found in Segura et al. [22].

3.1 Ground motion record selection method

To proceed with the vulnerability assessment of the dam considered in this study through the development of fragility functions, a representative set of ground motion time series (GMTS), which properly accounts for



the aleatory uncertainty, is necessary [23, 24]. The generalized conditional intensity measure (GCIM) approach [25] was adopted to select recorded GMTS due to its ability to include the most influencing seismic intensity measures with respect to the structural response. For the case of gravity dam-type structures, peak ground velocity (PGV) was found to be one of the best-performing structure-independent ground-motion scalar IMs to correlate with damage [26]. Similarly, besides the horizontal spectral acceleration (S_{aH}), the vertical spectral acceleration (S_{aV}) is also expected to be relevant in heavy structures of this type. As a result, the set of considered IMs in the GCIM is $\{S_{aH}(T); S_{aV}(T); PGV\}$, where $S_{aH}(T)$ and $S_{aV}(T)$ are computed at 20 vibration periods in the range of $T = [0, 2T_1 - 2T_1]$ as proposed by Baker [27]. The GCIM distribution computed using the abovementioned IMs was then used to simulate and select 250 ground motions. The records were selected from the PEER NGA-West2 database [28] due to the limited availability of strong ground motion records in the PEER NGA-East database [29]. Additional specifics on the record selection procedure can be found in Segura et al. [22].

4. Seismic analysis of the dam via surrogate model

The basic idea in the surrogate model approach is to avoid the temptation to invest computational budget in answering the question at hand and, instead, invest in developing fast mathematical approximations to the long running computer codes. As such, these models seek to provide answers in the gaps between the necessarily limited analysis runs that can be afforded with the available computing power. To reduce the computational expense, the surrogate acts as a "curve fit" to the available data so that results may be predicted without recourse to the use of the expensive simulation code. The meta-model considered herein is within an adaptive scheme, i.e., the functions in the meta-model can change according to the input data to reduce the burden of manual selection of several parameters in the meta-model. The surrogate modeling procedure comprises three major steps which may be interleaved iteratively: (i) sample selection (also known as sequential design, optimal experimental design or active learning), (ii) construction of the surrogate model and optimizing the model parameters (bias-variance trade-off) and (iii) appraisal of the accuracy of the surrogate [12].

4.1 Design of experiments (DOE)

To minimize the associated cost of running a dynamic non-linear FEM, an appropriate experimental design method, such as Latin Hypercube sampling (LHS), should be used. This design of experiments (DOE) technique has been widely adopted for deterministic computer experiments [30], wherein a particular combination of dam modeling parameters coupled with a ground motion record will yield the seismic response. The Latin Hypercube design divides the desired range for each element within the parameter vector p into n_f intervals of equal marginal probability $1/n_f$ and then selects a sample once from each interval. The selected n_f samples for the first factor (p_1) are combined with the n_f samples of the second factor (p_2), and subsequent factors ($p_3 \dots p_m$) such that it maximizes the minimum distance between the design points.

Table 1 presents the parameters, p_m , that were considered as random variables in the numerical analysis of the dam response and for which the uncertainty was formally included through their probability distribution function (PDF). All the remaining input parameters were kept constant and represented by their best estimate values. For the studied dam, owing to the limited availability of material investigations, the probability distributions were defined using the empirical data of similar dams. The uniform distribution was used for most parameters except for damping, for which a log-normal distribution was adopted as proposed by Ghanaat et al. [31].

Each row of the LHS experimental design matrix, \mathbf{X} is then paired with the n selected ground motions record with varying intensity measures. Hence, the dimensions of the original LHS experimental design matrix are $m \times n$. Besides the model parameters of Table 1, the seismic IMs listed in Table 2 were considered in the experimental design matrix.



Table 1 – Model parameters PDFs

| Parameters | PDF | PDF Parameters | |
|-----------------------------------------------|------------|-------------------|----------------|
| Concrete–rock tensile strength (MPa), CRT | Uniform | L = 0.2 | U = 1.5 |
| Concrete–concrete tensile strength (MPa), CCT | Uniform | L = 0.3 | U = 2.0 |
| Concrete–rock cohesion (MPa), CRC | Uniform | L = 0.3 | U = 2.0 |
| Concrete–concrete cohesion (MPa), CCC | Uniform | L = 0.9 | U = 2.5 |
| Concrete–rock angle of friction (°), CRF | Uniform | L = 42 | U = 55 |
| Concrete–concrete angle of friction (°), CCF | Uniform | L = 42 | U = 55 |
| Concrete damping (%), CD | Log-normal | $\lambda = -2.99$ | $\zeta = 0.35$ |
| Drain efficiency, DR | Uniform | L = 0.0 | U = 66 |

Table 2 – Seismic IMs considered in the experimental design matrix

| Seismic Intensity parameters | |
|-----------------------------------|------------------------------------------------------|
| S _{aH} (T ₁) | spectral acceleration at T ₁ |
| S _{vH} (T ₁) | spectral velocity at T ₁ |
| PGA | peak ground acceleration |
| PGV | peak ground velocity |
| PGD | peak ground displacement |
| SI | spectrum intensity |
| ω_{exp} | earthquake angular frequency |
| D ₅₉₅ | significant duration |
| I _a | Arias intensity |
| PGA _v | vertical peak ground acceleration |
| S _{aV} (T ₁) | vertical spectral acceleration at the T ₁ |

Given that 250 GMTS were selected, the original dimensions of the experimental design matrix were $\mathbf{X}[19 \times 250]$ to which mathematical transformations (natural logarithm, exponential form, etc.) and parameter product combinations were added. Finally, for each row, \mathbf{x}_i , of the experimental design matrix, $n_f = 250$ finite element simulations were conducted. The structural response, y_i , considered herein was the maximum relative sliding, δ_{max} . Hence a response vector $\mathbf{y}[250 \times 1]$ was obtained as a result of the FEM simulation, to be used to train the surrogate model.

4.1 Polynomial response surface meta-model

A polynomial response surface (PRS) is a regression technique where an n -dimensional surface that predicts desired responses is developed using a computationally efficient closed-form polynomial function developed from a set number of input variables [32]. The sparse polynomial response surface can be represented as:

$$y_i = \boldsymbol{\theta}^T g(\mathbf{X}) + v \quad (1)$$

where, y_i is the engineering demand parameter as a result of the finite element model simulation i , g is a column vector that includes explanatory functions that are powers and cross products of powers of the predictors in \mathbf{X} up to a predefined degree. $\boldsymbol{\theta}^T$ is the row vector of model parameters, which are unknown constant coefficients, and v is the model error due to the lack of fit of the surrogate model.

As it was aforementioned, the maximum relative sliding at the base was computed from non-linear simulations, and a polynomial response surface meta-models was trained to emulate the structural response.



Only the best demand and capacity predictors from the initial training set of explanatory functions were considered. To this end, the stepwise regression algorithm in MATLAB [33, 34] was used when fitting the meta-models. The algorithm starts with a constant term to predict the response. In the next step, one predictor is added to the model, and the performance of the model is evaluated based on the Bayesian information criterion (BIC) [33, 34]. If the model performance improves, the added term is kept; otherwise, it is removed, and this process is repeated until all the proposed predictors are tested. As a result of this process, the final set of explanatory functions in the final model is a subset of the initial set. The prediction accuracy of the developed models is evaluated with the 5-fold cross-validation method [12], and the average root mean square error (RMSE), relative maximum absolute error (RMAE) and coefficient of determination (R²) are used as the model goodness-of-fit. In addition to the 5-fold cross-validation method, p-values associated with the explanatory functions are controlled to be smaller than 0.05, assuring that the final terms included in the model are not selected by chance.

The final surrogate resulted in a polynomial response surface of order 4 (PRS-O4) as a function of three model parameters, three seismic intensity measures and their transformations and pairwise products.

$$\delta_{max} = g(\text{CRC}, \text{CRF}, \text{DR}, \text{PGV}, \text{Ia}, \text{PGA}_v) + v \quad (2)$$

$$v \sim \mathcal{N}(0, \sigma_v^2) \quad (3)$$

where CRC, CRF, DR are the model parameters corresponding to the concrete-rock cohesion, the concrete-rock angle of friction and drain efficiency, respectively; PGV is the peak ground velocity, PGA_v is the peak ground acceleration in the vertical direction and Ia is Arias intensity. A normally distributed model error term v , with zero mean and standard deviation equal to the RMSE is added to the selected surrogate model to contemplate the lack of fit. Fig. 2 (a) shows that the predicted values with the selected meta-model agree with the simulated dataset, while in Fig. 2 (b) it can be seen that the residual normal distribution error hypothesis is respected.

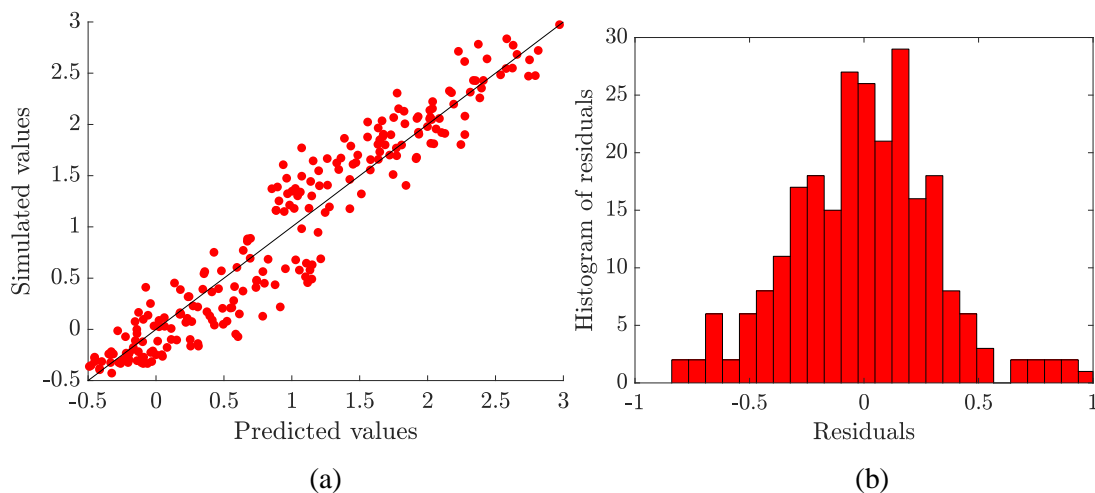


Fig. 2 – PRS-O4: (a) predicted vs. simulated values and (b) residuals histograms

5. Seismic fragility analysis

Earthquake shaking represents complex loading to a structure which cannot be accurately characterized by a single parameter such as peak ground acceleration [35]. The estimation of the fragility of the system can be potentially improved by increasing the number of parameters. Noted advantages of these parameterized or



multivariate fragility functions include the potential for efficient definition of the seismic scenario and exploring sensitivities or the influence of seismic parameter variation.

Similar to fragility curves, multivariate fragility functions offer the conditional probability of exceeding different limit states given the occurrence of an earthquake of a certain intensity. The only difference is that the specific limit state is characterized with n parameters p_1, p_2, \dots, p_n instead of one parameter, as is the case with fragility curves. Hence the probability of limit state exceedance is conditioned on the resulting set of critical parameters. The fragility function corresponding to the limit state l is defined as follows:

$$F_l(x_1, x_2, \dots, x_n) = P_f(\text{LS} \geq \text{LS}_l | p_1 = x_1, p_2 = x_2, \dots, p_n = x_n) \quad (4)$$

where LS is the limit state damage index, and LS_l is the value corresponding to the l^{th} limit state. While fragility curves are usually represented by well-known and readily parameterizable probability distributions like the log-normal one, the problem gets more complex for surfaces, where bivariate distributions must be computed.

5.1 Damage states

When subjected to strong ground motion, gravity dams may be damaged in different ways. In recent years, typical damage modes that could lead to the potential collapse of dams after a seismic event have been identified, and seismic damage levels have been established [36, 37]. Preliminary analyses have identified sliding as the critical failure mode for the case study dam [16], and other failure modes would only occur after sliding has already been observed. As a result, the concrete-to-rock sliding at the base of the dam interface was considered in this study. Each limit state was characterized by the sliding damage states presented in Table 3.

Table 3 – Limit states for the case study dam

| Sliding damage state | Base |
|----------------------|--------|
| LS0 - Slight | 5 mm |
| LS1 - Moderate | 25 mm |
| LS2 - Extensive | 50 mm |
| LS3 - Complete | 150 mm |

5.2 Sample generation and fragility point estimates

Given the number of simulations required to generate a fragility surface, instead of nonlinear dynamic analysis the results from the meta-models were used to generate the fragility point estimates. Regarding the generation of the samples where the meta-model will be evaluated to predict the dam's response, independence between all the modeling parameters was considered to generate 5×10^5 samples with LHS. The values of the seismic IMs were bounded, as shown in Table 4, to efficiently cover the range of values corresponding to return periods from 700–30000 years.

Table 4 – Seismic IMs range of values

| Intensity measures | Range of values |
|--------------------|-----------------|
| PGV | 0.8–25.0 cm/s |
| Ia | 0.0–2.5 m/s |
| PGA _v | 0.01–0.25 g |



To generate point fragility estimates from the metamodels, a sampling strategy that draws upon the approach presented in multiple stripe analysis (MSA) [38] is adopted, where both ground motion IM ranges are stratified. To this end, the two selected IMs are divided in N and M intensity levels, and samples are generated as shown in Fig. 3. While keeping one parameter constant, the other is varied among the different levels, and its response is approximated with the surrogate. The point fragility estimate is calculated as the number of samples with specific IMs intensity level that exceed a determined limit state over the total number of samples generated with those specific IMs. The range of each of the parameters of the fragility surface was divided in 100 intervals, resulting in the generation of 10^4 fragility point estimates for each limit state.

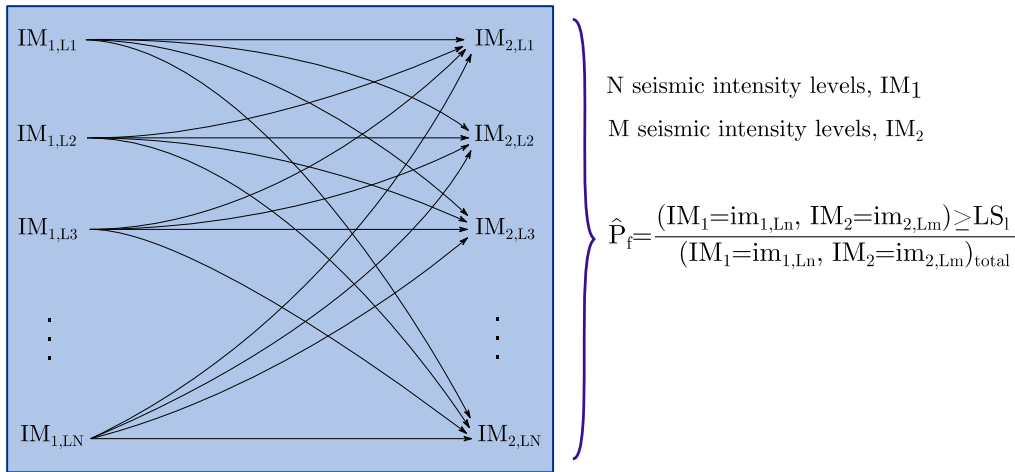


Fig. 3 – Multiple stripe analysis for meta-model fragility point estimate generation

5.3 Fragility surface generation

In the context of this study, point fragility estimates were generated as a function of PGV and I_a , the two most influential seismic IMs from stepwise regression. The uncertainty due to all other parameters involved in the meta-model response is propagated in the analysis by sampling these parameters with LHS according to their respective range of usable values (Table 2 and Table 4). In order to fit parametrized surfaces to the point fragility estimates, the methodology proposed by Baker [38] for the efficient fitting of fragility curves, was extrapolated to fit fragility surfaces. It was assumed that for each LS, the fragility surface is described by the product of two independent cumulative distribution functions (CDF), as presented in Eq. 5,

$$F_S(PGV, I_a) = \Phi_{PGV}(PGV, \theta_{PGV}, \beta_{PGV}) \Phi_{I_a}(I_a, \theta_{I_a}, \beta_{I_a}) \quad (5)$$

where after testing several distributions Φ_{PGV} and Φ_{I_a} are normal CDFs and θ_{PGV} , β_{PGV} , and θ_{I_a} , β_{I_a} and are the parameters characterizing each respective CDFs. The parameters of each fragility surface were estimated with the MLE method as proposed by Baker [38], when using the MSA for efficient fragility functions' fitting and can be found in Table 5. As it can be seen in Fig. 4 and from Table 6, the parametric fragility surfaces fit well the fragility estimates calculated with the meta-model and describe well the behavior of the structure with increasing levels of the selected seismic intensity measures.

Table 5 – PGV- I_a fragility surfaces parameters

| Limit state | θ_{PGV} | β_{PGV} | θ_{I_a} | β_{I_a} |
|-------------|----------------|---------------|----------------|---------------|
| LS0 | -0.643 | 9.340 | 0.039 | 0.643 |
| LS1 | 10.189 | 15.954 | 0.623 | 0.641 |
| LS2 | 20.606 | 22.146 | 0.804 | 0.614 |
| LS3 | 61.760 | 42.983 | 1.024 | 0.554 |



Table 6 – PGV-Ia fragility surfaces goodness-of-fit

| Limit state | R ² | RMSE | RMAE |
|-------------|----------------|-------|-------|
| LS0 | 0.947 | 0.043 | 1.184 |
| LS1 | 0.988 | 0.018 | 0.484 |
| LS2 | 0.984 | 0.014 | 0.564 |
| LS3 | 0.961 | 0.008 | 1.238 |

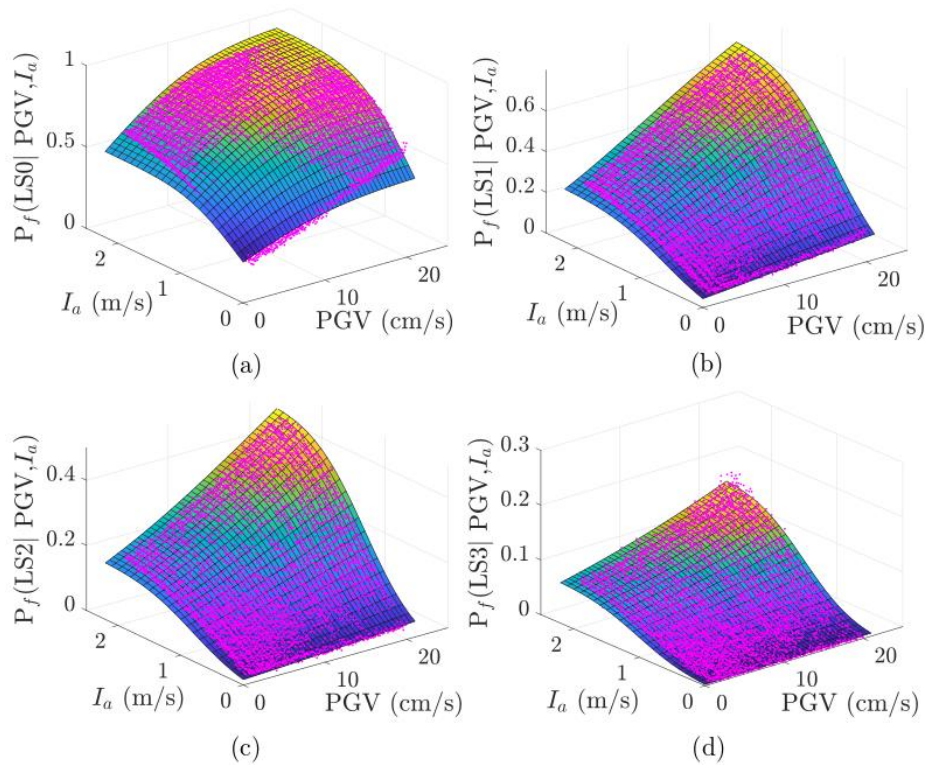


Fig. 4 – Fragility surfaces for (a) LS0, (b) LS1, (c) LS2 and (d) LS3

5.3 Fragility functions comparison

Fragility curves were also generated for the case study dam as a function of PGV to compare the variability of the fragility estimates coming from univariate and bivariate seismic fragility functions. The fragility curves were generated in the same manner as the fragility surfaces, but in this case the uncertainty in the modeling parameters and in the seismic IMs not explicitly shown in the curve, was propagated in the analysis by sampling from the range of possible values as shown in Table 2 and 4.

In the same manner, and to illustrate the aforementioned robustness of the fragility assessment using univariate functions, Fig. 5 shows the fragility curves for each limit state in red, and the shaded areas represent the fragility curves generated by intersecting the surfaces of Fig. 4 with two vertical planes at $I_a=0.0$ m/s and $I_a=2.5$ m/s (Table 4). It can be seen that for LS0, LS1 and LS2, the fragility curve is closer to the fragility estimates obtained with high I_a values which, for high PGV values, can lead to an unrealistic seismic scenario and to an overly conservative probability of exceeding a determined LS.

6. Conclusions

The main objective of this study was to generate seismic fragility surfaces for assessing in a more efficient way the seismic safety of gravity dam-type structures, developed by the implementation of a surrogate model. The proposed methodology was applied to a case study dam in Quebec which presents a well-documented dynamic behavior.



A polynomial response surface meta-model was trained to fit the seismic response of the studied dam, selecting as engineering demand parameter the maximum relative sliding at the base of the dam. The 250 GMTS used for the analysis were selected with the GCIM method including the results of the PSHA performed at the dam site. This meta-model was used to generate fragility surfaces as a function of two seismic IMs. The fragility point estimates were generated as a function of PGV and I_a , the two most influential seismic IMs. The uncertainty due to the modeling parameters and PGA_V was propagated in the analysis by sampling these parameters with LHS according to their respective range of usable values.

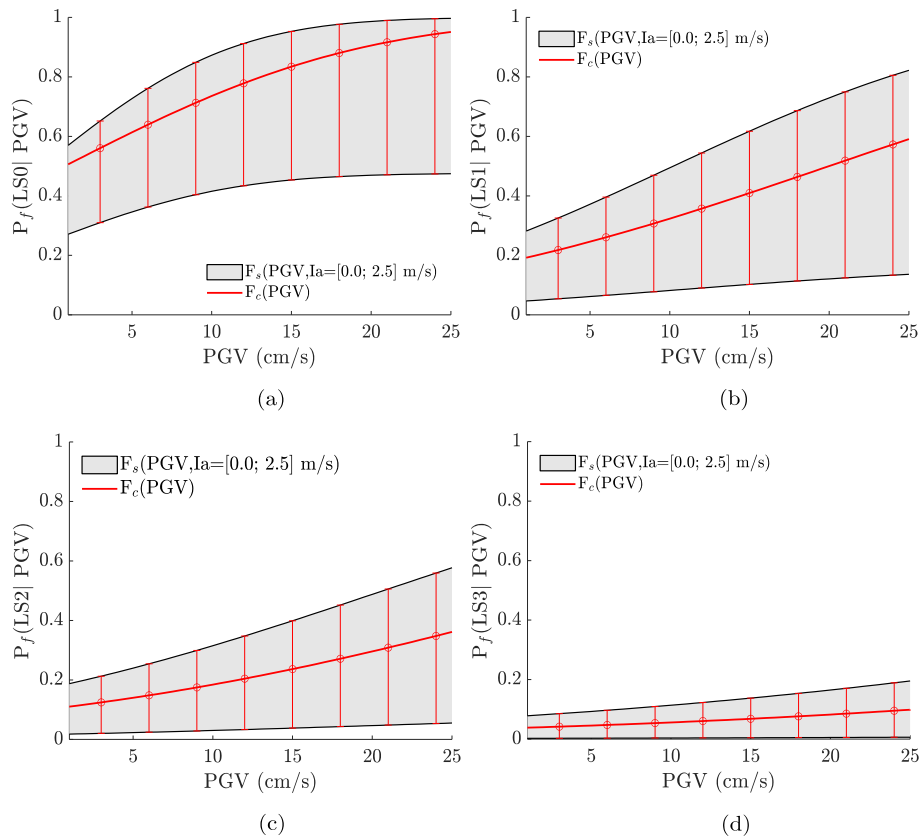


Fig. 5 – Fragility curves comparison for (a) LS0, (b) LS1, (c) LS2 and (d) LS3

It was assumed that for each limit state, the fragility surface is described by the product of two independent normal cumulative density functions. It was observed that the parametric fragility surfaces fit well the fragility estimates calculated with the meta-model and describe well the behavior of the structure with increasing levels of the selected seismic intensity measures. Likewise, fragility curves as a function of PGV were generated by propagating the uncertainty of the parameters affecting the surrogate model and by considering the extreme values of the usable range of I_a values. It was observed that for most LS the obtained fragility curve is closer to the upper bound of the fragility region resulting from the I_a extreme values, evidencing an estimation robustness that is highly dependent on the selected IM. Consequently, the fragility surface offers a more complete and accurate view of the vulnerability of the structure. Such fragility surfaces can be implemented within earthquake risk evaluation tools and they should provide more precise damage estimations. However, it should be mentioned that even if a fragility surface allows considering more general cases and a more efficient definition of the seismic demand, using two (usually) correlated seismic IMs to build the fragility surface, can lead to the consideration of seismic scenarios very unlikely to happen at the site of the structure during its lifetime.



7. Acknowledgments

The authors acknowledge the financial support of Mitacs, the Natural Sciences and Engineering Research Council of Canada (NSERC), the Fonds de recherche du Québec – Nature et technologies (FRQNT), the Centre d'études interuniversitaire des structures sous charges extrêmes (CEISCE) and the Centre de recherche en génie parasismique et en dynamique des structures (CRGP). Computational resources for this project were provided by Compute Canada and Calcul Québec. Any opinions, findings, and conclusions or recommendations expressed in this paper are those of the authors and do not necessarily reflect the views of the sponsors.

8. Copyrights

17WCEE-IAEE 2020 reserves the copyright for the published proceedings. Authors will have the right to use content of the published paper in part or in full for their own work. Authors who use previously published data and illustrations must acknowledge the source in the figure captions.

9. References

- [1] United States Society of Dams, U.S.S.D. (2014): Observed Performance of Dams During Earthquakes, volume III.
- [2] Wieland M (2013): Seismic design of major components. *International Water Power*. <http://www.waterpowermagazine.com/features/featureseismic-design-of-major-components>.
- [3] Marche C (2008): Barrages, crues de rupture et protection civile. *Presses internationales Polytechnique*, 2 edition.
- [4] Lave LB, Resendiz-Carrillo D, McMichael FC (1990): Safety goals for high-hazard dams: are dams too safe? *Water Resources Research*, **26**,1383–1391.
- [5] Schultz MT, Gouldby BP, Simm JD, Wibowo JL (2010): Beyond the factor of safety: Developing fragility curves to characterize system reliability. *Technical report ERDC SR-10-01*, U.S. Army Corps of Engineers.
- [6] Tekie PB, Ellingwood BR (2002): Fragility analysis of concrete gravity dams. *Journal of infrastructure systems*, **127** (8), 41–48.
- [7] Alembagheri M (2018): Investigating Efficiency of Vector-Valued Intensity Measures in Seismic Demand Assessment of Concrete Dams. *Advances in Civil Engineering*, 2018:12.
- [8] Ghosh J, Padgett JE, Dueñas Osorio L (2013): Surrogate modeling and failure surface visualization for efficient seismic vulnerability assessment of highway bridges. *Probabilistic Engineering Mechanics*, **34**, 189–199.
- [9] Hariri-Ardebili MA, Saouma V (2016): Seismic fragility analysis of concrete dams: A state-of-the-art review. *Engineering Structures*, **128**, 374–399.
- [10] Baker JW, Cornell C (2006): Vector-Valued Ground Motion Intensity Measures for Probabilistic Seismic Demand Analysis. *PEER 2006/08*, Technical report.
- [11] Tothong P, Luco N (2007): Probabilistic seismic demand analysis using advanced ground motion intensity measures. *Earthquake engineering & Structural dynamics*, **36** (13), 1837–1860.
- [12] Forrester AIJ, Sóbester A, Keane AJ (2008): Engineering Design via Surrogate Modelling: A practical Guide. *Wiley*.
- [13] Proulx J, Paultre P (1997): Experimental and numerical investigation of dam-reservoir-foundation interaction for a large gravity dam. *Canadian Journal of Civil Engineering*, **24**, 90–105.
- [14] Mills-Bria B, Koltuniuk R, Percell P (2013): State-of-Practice for the Nonlinear Analysis of Concrete Dams 2013. Technical report, *U.S Department of the interior Bureau of Reclamation*.
- [15] Livermore Software Technology Corporation, LSTC (2013): LS-Dyna R9.1.0, *software*.
- [16] Bernier C, Padgett JE, Proulx J, Paultre P (2014): Seismic fragility of concrete gravity dams with modeling parameter uncertainty and spacial variation. *ASCE Journal of Structural Engineering*, **142** (5), 05015002.



- [17] Segura RL, Bernier C, Durand C, Paultre P (2019): Modelling and Characterizing a Concrete Gravity Dam for Fragility Analysis. *Infrastructures*, **4** (62), 1–19.
- [18] Natural Resources Canada, NRC (2015): Simplified seismic hazard map for Canada. <http://www.earthquakecanada.nrcan.gc.ca/hazard-alea/simphaz-eng.php>. Visited on 2016-02-08.
- [19] Halchuk S, Allen T, Adams J, Rogers G (2014): Fifth Generation Seismic Hazard Model Input Files as Proposed to Produce Values for the 2015 National Building Code of Canada. *Technical Report Open File 7575*, Geological Survey of Canada.
- [20] Atkinson G, Adams J (2013): Ground motion prediction equations for application to the 2015 Canadian national seismic hazard maps. *Canadian Journal of Civil Engineering*, **40**, 988–998.
- [21] Global Earthquake Model Foundation, GEM (2015): OpenQuake Engine 2.8, *software*.
- [22] Segura RL, Bernier C, Monteiro R, Paultre P (2018): On the seismic fragility assessment of concrete gravity dams in eastern Canada. *Earthquake Spectra*, **35** (1), 211–231.
- [23] Padgett JE, DesRoches R (2007): Sensitivity of Seismic Response and Fragility to Parameter Uncertainty. *Journal of Structural Engineering*, **133**, 1710–1718.
- [24] Haselton CB, Baker JW, Bozorgnia Y, Goulet CA, Kalkan E, Luco N, Shantz T, Shome N, Stewart JP, Tothong P, Watson-Lamprey J, Zareian F (2009): Evaluation of Ground Motion Selection and Modification Methods: Predicting Median Interstory Drift Response of Buildings. *PEER 2009/01*, Technical report.
- [25] Bradley BA (2010): A generalized conditional intensity measure approach and holistic ground motion selection. *Earthquake Engineering and Structural Dynamics*, **56**, 1321–1342.
- [26] Hariri Ardebili MA, Saouma V (2016): Probabilistic seismic demand model and optimal intensity measure for concrete dams. *Structural Safety*, **59**, 67–85.
- [27] Baker JW (2011): Conditional mean spectrum: Tool for ground-motion selection. *Journal of Structural Engineering*, **220**, 1–8.
- [28] Ancheta TD, Darragh RB, Stewart JP, Seyhan E, Silva WJ, Chiou KE, Brian SJ, Wooddell Graves RW, Kottke AR, Boore DM, Kishida T, Donahue JL (2013): PEER NGA-West2 Database. *PEER 2013/03*, Technical report.
- [29] Goulet CA, Kishida T, Ancheta TD, Cramer CH, Darragh RB, Silva WJ, Hashash Y, Harmon J, Stewart JP, Wooddell KE, Youngs RR (2014): PEER NGA-East Database. *PEER 2014/17*, Technical report.
- [30] Hariri-Ardebili MA (2018): MCS-based response surface metamodelling and optimal design of experiments for gravity dams. *Structure and infrastructure engineering*, **2479**, 1–23.
- [31] Ghanaat Y, Patev RC, Chudgar AK (2012): Seismic fragility analysis of concrete gravity dams. *15th World Conference on Earthquake Engineering*, Lisbon.
- [32] Murphy KP (2012): Machine Learning A Probabilistic Perspective. *The MIT Press*, Cambridge, UK.
- [33] Collett D, (2002): Modeling Binary Data. *Chapman & Hall/CRC*.
- [34] Dobson AJ, (1990): An Introduction to Generalized Linear Models. *Chapman & Hall/CRC*.
- [35] Seyedi DM, Gehl P, Douglas P, Davenne L, Mezher N, and Ghavamian S (2010): Development of seismic fragility surfaces for reinforced concrete buildings by means of nonlinear time-history analysis. *Earthquake Engineering and Structural Dynamics*, **39** (1), 91–108.
- [36] Hariri-Ardebili MA, Saouma V (2015): Quantitative failure metric for gravity dams. *Earthquake Engineering & Structural Dynamics*, **44**, 461–480.
- [37] Lupoi A, Callari C (2013). A probabilistic method for the seismic assessment of existing concrete gravity dams. *Structure and Infrastructure Engineering: Maintenance, Management, Life-Cycle Design and Performance*, **8** (2013), 37–41.
- [38] Baker JW (2015): Efficient analytical fragility function fitting using dynamic structural analysis. *Earthquake Spectra*, **31**, 579–599.